

Reducing Global Turbulent Resistivity by Eliminating Large Eddies in a Spherical Liquid-Sodium Experiment

E. J. Kaplan,^{1,2} M. M. Clark,^{1,2} M. D. Nornberg,^{1,2} K. Rahbarnia,^{1,2} A. M. Rasmus,^{1,2} N. Z. Taylor,^{1,2}
C. B. Forest,^{1,2,*} and E. J. Spence^{2,3}

¹*Department of Physics, University of Wisconsin–Madison, 1150 University Avenue, Madison, Wisconsin 53706, USA*

²*Center for Magnetic Self Organization in Laboratory and Astrophysical Plasmas*

³*Princeton Plasma Physics Laboratory, P.O. Box 451, Princeton, New Jersey 08543, USA*

(Received 21 January 2011; revised manuscript received 5 May 2011; published 21 June 2011)

Three-wave turbulent interactions and the role of eddy size on the turbulent electromotive force are studied in a spherical liquid-sodium dynamo experiment. A symmetric, equatorial baffle reduces the amplitude of the largest-scale turbulent eddies, which is inferred from the magnetic fluctuations spectrum (measured by a 2D array of surface probes). Differential rotation in the mean flow is >2 times more effective in generating mean toroidal magnetic fields from the applied poloidal field (via the Ω effect) when the largest-scale eddies are eliminated, thus demonstrating that the global turbulent resistivity (the β effect from the largest-scale eddies) is reduced by a similar amount.

DOI: 10.1103/PhysRevLett.106.254502

PACS numbers: 47.65.-d, 47.27.-i, 91.25.Cw, 96.60.Hv

The magnetic fields of stars and planets are generated by the dynamo effect—a magnetohydrodynamic instability in flowing conducting fluids that converts kinetic flow energy into magnetic energy. Experimental demonstrations of dynamos have been achieved in heavily constrained flows [1,2] as well as in simple roll flows with nonuniform magnetic diffusivities [3].

Magnetic field dynamics are governed by the magnetic induction equation

$$\frac{\partial \mathbf{B}}{\partial t} = Rm \nabla \times (\mathbf{v} \times \mathbf{B}) + \nabla^2 \mathbf{B}, \quad (1)$$

where $Rm = \mu_0 a v / \eta$ is the magnetic Reynolds number with a the system scale, v the characteristic velocity, and η the resistivity. Time is scaled to the resistive diffusion time $\tau_\eta = \mu_0 a^2 / \eta$. A magnetic field can be generated from a flowing liquid metal or plasma when advection dominates diffusion sufficiently to amplify magnetic perturbations ($Rm \gg 1$) and when the flow geometry provides a feedback mechanism to facilitate instability.

A key component of most dynamo theories is that correlated fluctuations of velocity and magnetic fields ($\tilde{\mathbf{v}}$ and $\tilde{\mathbf{b}}$, respectively) can generate, on average, a turbulent electromotive force $\langle \tilde{\mathbf{v}} \times \tilde{\mathbf{b}} \rangle$ that drives a mean-field current. This effect is often quantified in terms of transport coefficients α and β such that $\langle \tilde{\mathbf{v}} \times \tilde{\mathbf{b}} \rangle = \alpha \langle \mathbf{B} \rangle - \beta \nabla \times \langle \mathbf{B} \rangle$, where the brackets denote a time average [4].

The effective resistivity for turbulent flows is enhanced by the magnetic flux transport and mixing by eddies. By assuming isotropic and homogeneous turbulence, zero mean flow, and scale separation between the small turbulence and the system-scale magnetic field, the mean-field theory shows that the enhanced resistivity can be characterized as $\eta_{\text{eff}} = \eta + \eta_{\text{turb}}$ with $\eta_{\text{turb}} \sim \frac{1}{3} Rm_{\text{turb}} \eta$ [5]. Here we have defined a turbulent magnetic Reynolds

number $Rm_{\text{turb}} \equiv \mu_0 \tilde{v} \ell / \eta$, where \tilde{v} is the rms velocity fluctuation level and $\ell = \tilde{v} \tau_{\text{corr}}$ is the characteristic scale length of the eddies. This turbulent resistivity is often the dominant contribution in astrophysical dynamos as Rm_{turb} is usually enormous; e.g., the resistive decay time of the Sun is 10^7 times larger than predicted by Spitzer conductivity [6,7].

In real systems the largest eddies often carry the most turbulent energy. These large eddies are strongly affected by the geometry and have a similar scale as the magnetic field. These large-scale eddies can also greatly reduce the effective Rm of the system-scale flow [$Rm_{\text{eff}} = Rm(\eta/\eta_{\text{eff}})$], thereby raising the dynamo excitation threshold as observed in several low magnetic Prandtl number simulations of dynamo experiments [8–10]. These numerical studies predict that large-scale fluctuations are more detrimental to dynamos than those at small scales [8]. This suppression is consistent with a global β effect. Turbulent effects were evidently unimportant in determining the self-excitation threshold in two early dynamo experiments, quite likely because scale separation was enforced. Eddy scales were set by the transverse dimensions of the pipes used to guide the flow [1,2], and the β effect was minimized.

In this Letter, we report on changes to the turbulence-induced fields in the Madison dynamo experiment (MDE) when the largest-scale eddies are suppressed. We also provide a method of understanding this change in terms of nonlinear three-wave couplings in a sphere. Previous Letters have reported evidence for mean-field currents in the unconstrained geometry of the MDE: a turbulence-generated dipole moment was observed (which we will refer to as a global α effect) [11], and the field line stretching by shear flow was inhibited (which we will refer to as a global β effect, or enhanced diffusivity) [12]. Other

recent experiments (in Perm and at New Mexico Tech) have also inferred or directly measured the turbulent resistivity [13,14]. Here, we present evidence that the introduction of a baffle at the equator of the sphere has eliminated these effects by suppressing the culpable large-scale eddies.

The MDE is 0.5 m radius sphere filled with liquid sodium. Two 75 kW motors turn a pair of 30 cm impellers to generate a two-vortex flow with the symmetry axis collinear with the motor shafts. A simulation of the flow is shown in Fig. 1. An array of 74 Hall probes at the surface measures the radially directed component of the magnetic field with a resolution of 0.25 G. Five radial arrays of 3-*d* Hall probes measure internal fields resolved to 1.0 G. External electromagnets can apply four distinct magnetic configurations—axial dipole, axial quadrupole, transverse dipole, and transverse quadrupole—with field strengths ranging from 0 to 100 G.

The spherical geometry of the MDE allows a convenient representation of incompressible vector fields by orthogonal toroidal and poloidal basis functions, e.g.,

$$\mathbf{B} = \sum_i \nabla \times \nabla \times S_{l_i}^{m_i}(r) Y_{l_i}^{m_i}(\theta, \phi) \hat{\mathbf{r}} + \nabla \times T_{l_i}^{m_i}(r) Y_{l_i}^{m_i}(\theta, \phi) \hat{\mathbf{r}},$$

where magnetic fields are denoted by *T* and *S* and flows by *t* and *s*. We assume that the vector fields can be further separated into mean and fluctuating components, e.g., $S_1^1 = \langle S_1^1 \rangle + \tilde{S}_1^1$. The axisymmetric two-vortex flow of Fig. 1 consists predominantly of $\langle t_2^0 \rangle \langle s_2^0 \rangle$ as originally motivated by several theoretical studies [15]. This formalism [16] provides a natural set of basis functions for inferring properties of the turbulent flow from the measurements of the induced magnetic field. Three-mode

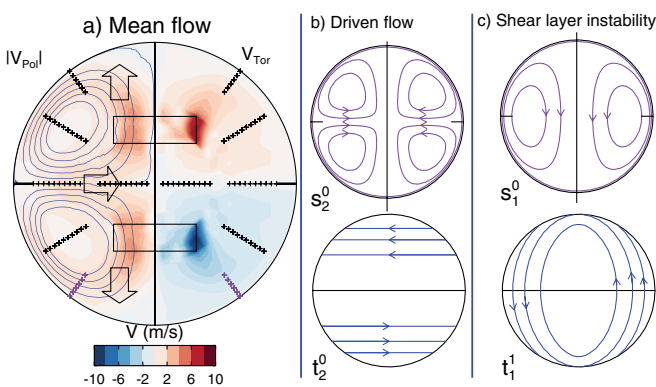


FIG. 1 (color online). (a) Mean internal flow for the Madison dynamo experiment. The hollow black boxes represent the 30 cm impellers, and the short, thick black lines represent the 8 cm baffles. The flows are computed by using ANSYS® FLUENT® for flows with impellers rotating at 800 rpm. The internal probe array is indicated by the black and purple crosses (purple crosses being the locations of the probes in Fig. 4). The right side of the figure shows the (b) driven and (c) lowest-order fluctuating flows.

interactions are represented as $B_{l_i}^{m_i} \xrightarrow{v_{l_j}^{m_j}} B_{l_k}^{m_k}$; i.e., the magnetic mode *i* interacts with the flow *j* to produce the magnetic mode *k*. The evolution of a given magnetic mode *B_k* is given by the total of three-wave couplings between the flow and full magnetic field:

$$\partial_t B_k = \frac{\eta}{\mu_0} \left(\frac{\partial^2}{\partial r^2} - \frac{p_k}{r^2} \right) B_k + \sum_{i,j} B_i \xrightarrow{v_j} B_k. \quad (2)$$

Here, $p_k = l_k(l_k + 1)$. A graphical representation of the lowest-order couplings and selection rules is shown in Fig. 2. The experimental technique employed to infer properties of the flow is to apply an external magnetic field and measure the response field. The three applied field configurations correspond to S_1^0 , S_1^1 , and S_2^0 poloidal magnetic fields. The surface probe array can resolve poloidal spherical harmonics of the emerging magnetic field up to a polar order of $l = 7$ and $m = 5$ through a singular value decomposition of the measured surface field.

The largest-scale fluctuations in the flow give rise to a nonlinear transfer of energy from the largest-scale magnetic fields to other modes in a process that resembles the conventional β effect. This comes about from bidirectional couplings in the bubble diagram, e.g., $\langle S_1^0 \rangle \xrightarrow{\tilde{t}_1^1} \tilde{S}_1^1 \xrightarrow{\tilde{t}_1^1} \langle S_1^0 \rangle$, that take the form

$$\partial_t \langle S_j \rangle = -\frac{p_j}{r^2} \langle S_j \rangle \sum_{i,k} \frac{L_{ijk} p_k}{N_j N_k r^2} \langle \tilde{t}_i^j \rangle \tau_{\text{corr},i}, \quad (3)$$

where L_{ijk} is the Elsasser integral, N_i is the normalization constant for the spherical harmonic, and $\tau_{\text{corr},i}$ is the auto-correlation time of the *i*th fluctuation. A similar result can be found for $\langle T_j \rangle$ modes. This nonlinear transfer

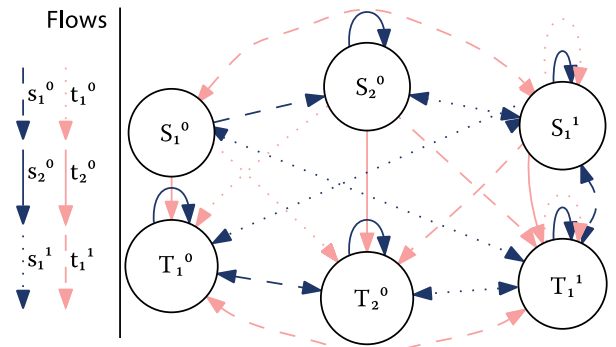


FIG. 2 (color online). Coupling of low-order magnetic modes by low-order flows. The circles contain magnetic modes, and the arrows represent the three-wave couplings between modes, their direction, and the flows that catalyze them. Only $S_{l_i}^{m_i}$ modes are observable on the surface of a sphere. The solid lines represent the mean flow in the MDE. The dashed lines are the large-scale fluctuations which are disrupted by the baffle. The dotted lines are the large-scale fluctuations which do not cross the baffle. The dynamo cycle based on the $\langle t_2^0 \rangle \langle s_2^0 \rangle$ flow, which connects S_1^1 , T_1^1 , S_2^0 , and T_2^0 , is not shown here.

when summed over all fluctuations resembles a turbulent diffusivity

$$\eta_{\text{turb},j} = \sum_{i,k} \frac{L_{ijk}^2 P_k}{N_j N_k r^2} \langle \tilde{t}_i^2 \rangle \tau_{\text{corr},i}. \quad (4)$$

A similar calculation for flows with turbulent helicity $\langle \tilde{v} \cdot \nabla \times \tilde{v} \rangle$ leads to a global α effect. In the spherical harmonic formalism, correlations between toroidal and poloidal fluctuations of identical mode numbers can convert a mean toroidal field into a mean poloidal field

$$\begin{aligned} \partial_t \langle S_j \rangle &= \langle T_i \rangle \sum_{m,n,k} (L_{nik} L_{mkj} + L_{mik} L_{nkj}) \\ &\times \frac{P_m P_k}{N_j N_k r^4} \langle \tilde{t}_n \tilde{s}_m \rangle \tau_{\text{corr},m,n}. \end{aligned} \quad (5)$$

If $n = m$, then $i = j$. This means that poloidal field is being driven by currents parallel to the toroidal magnetic field. It is natural to refer to this term as a global α effect with transport coefficient

$$\alpha_j = - \sum_{n,k} 2 \frac{L_{nik}^2 P_n P_k}{N_j N_k r^4} \langle \tilde{s}_n \tilde{t}_n \rangle \tau_{\text{corr},n}. \quad (6)$$

Previous results from the experiment are characterized by strong Kolmogorov-like turbulence for the smallest scales of the flow and low-frequency oscillations of the shear layer about the equatorial plane at the largest scale [17]. This hydrodynamic instability has been studied extensively in topologically similar turbulent flows [18,19] and is characterized mostly by fluctuations in the \tilde{t}_1^1 and \tilde{s}_1^0 spectral components of the flow, shown in Fig. 1. These spectral components have a characteristic scale of the order of the sphere radius and are larger in scale than the impeller driven vortices. We speculate that shear-layer fluctuations are responsible for increasing the volume-averaged effective resistivity by a factor of 2 [12].

In recent experiments, an axisymmetric stainless steel equatorial baffle has been installed that extends 8 cm inward from the wall. The baffle greatly reduces the

amplitude of the \tilde{t}_1^1 and \tilde{s}_1^0 fluctuations without significantly changing the magnetic boundary conditions, allowing the study of their role in the turbulent electromotive force. An estimate of the effect of the baffles on turbulent fluctuations comes from the turbulent dissipation of applied motor power $\epsilon \sim P/\rho \frac{4\pi}{3} a^3 \sim v_{\text{rms}}^3/a$, with P being the motor power, ρ the density, a the sphere radius, and v_{rms} the speed of turbulent fluctuations [20]. Here, a 20% reduction in motor power, such as we have for impellers rotating at 1000 rpm, corresponds to a 15% reduction in v_{rms}^2 . The reduction of the shear-layer fluctuations by an equatorial baffle has been directly observed in a similar geometry of the von Kármán flow in water experiments [18,19].

The addition of the equatorial baffle has eliminated the largest-scale eddies in the MDE.—Figure 3 shows a reduction of the fluctuation levels of the $\langle S_1^0 \rangle \xrightarrow{\tilde{s}_1^0} \tilde{S}_2^0$ [Fig. 3(b)], $\langle S_1^1 \rangle \xrightarrow{\tilde{t}_1^1} \tilde{S}_2^1$ [Fig. 3(h)], and $\langle S_2^0 \rangle \xrightarrow{\tilde{s}_2^0} \tilde{S}_3^0$ [Fig. 3(j)] interactions by $\sim 80\%$. In the Bullard-Gellman formulation, the \tilde{s}_1^0 flow is the only direct catalyst for these interactions. There is a similar reduction of $\langle S_1^1 \rangle \xrightarrow{\tilde{t}_1^1} \tilde{S}_1^1$ [Fig. 3(f)] and $\langle S_2^0 \rangle \xrightarrow{\tilde{t}_1^1} \tilde{S}_2^1$ [Fig. 3(l)]. Figure 1 shows that both the s_1^0 and t_1^1 eddies would flow across the equatorial baffle; note that they are the most significantly damped modes and that higher order fluctuations which result from smaller scales are relatively unaffected.

The elimination of the large-scale eddies has increased the Rm_{eff} to ~ 2.4 of its previous value.—The reduction in \tilde{t}_1^1 demonstrated in Fig. 3 would have an associated reduction in the η_{turb} of Eq. (4). The Ω effect, facilitated by the $\langle \tilde{t}_2^0 \rangle$ flow in the experiment, is the generation of a toroidal magnetic field from poloidal by differential rotation. The induced toroidal field serves as a measure of Rm_{eff} , since $B_\phi \sim Rm_{\text{eff}} B_0$, with B_0 the applied field strength [14]. Figure 4 shows a comparison of the toroidal windup as a function of radius in the region of the flow with the greatest differential rotation. The addition of the baffles has increased this windup factor by 2.36 ± 0.08 . Furthermore, the reduction of η_{turb} allows the mean

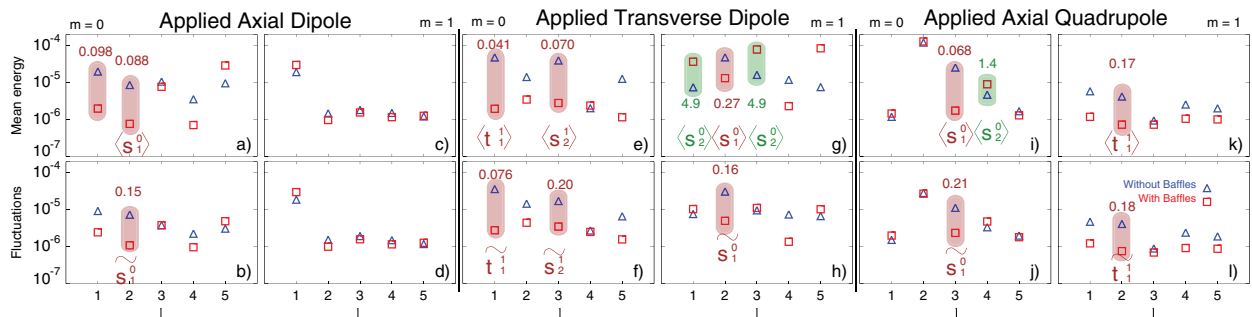


FIG. 3 (color online). Mean (a),(c),(e),(g),(i),(k) and fluctuating (b),(d),(f),(h),(j),(l) energies of the lowest-order poloidal harmonics at the sphere's surface. (a) and (b) describe the axisymmetric ($m = 0$) response to an axisymmetric applied magnetic dipole. (c) and (d) describe the transverse ($m = 1$) response. (e)–(h) repeat the same for an applied transverse magnetic dipole and (i)–(l) for an applied axial quadrupole. The induced fields are measured for impellers driven at 1000 rpm. Written above certain modes are the ratios of mode energies with and without baffles. Where applicable, the shortest interaction path from the applied to the response mode is indicated. Energies are integrated over free space and normalized to the internal energy of the applied magnetic field.

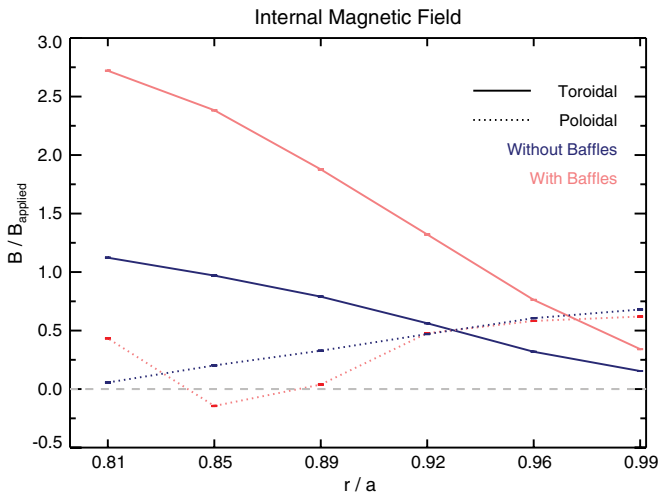


FIG. 4 (color online). Comparison of the toroidal gain and poloidal flux expulsion between 1000 rpm shots with and without baffles. The radial position is scaled with the radius of the sphere. Measured fields are scaled with the applied axial dipole field of 60 G. The probes are located at $\theta = 2.49$ and show the highest induced toroidal field in the sphere. Only the B_θ component of the poloidal field is shown.

flow to more effectively amplify and transport magnetic field. Figure 3(g) shows that the $\langle S_1^1 \rangle \xrightarrow{\langle S_2^0 \rangle} \langle S_3^1 \rangle$ interaction has been enhanced by the addition of baffles. This additional windup might be attributed in part to a change in the profile of the mean flow, which is not yet directly measured in the sodium experiment. However, since $\langle S_2^0 \rangle \xrightarrow{\langle S_3^0 \rangle} \langle S_4^0 \rangle$ was much more weakly affected, we conclude that the β effect must dominate.

The addition of the baffle has eliminated the α -effect-induced dipole moment.—The α effect of Eq. (6) is driven by correlated \tilde{r}_1^1 and \tilde{s}_1^1 flows. The elimination of either component would eliminate the α effect. Figure 3(a) shows that the mean dipole moment has weakened by an order of magnitude. The \tilde{s}_1^1 flow does not cross the baffle and may be unimpeded. However, the reduction of the \tilde{r}_1^1 flow is well established by the results presented in Fig. 3 and is sufficient to interrupt the loop.

The results presented demonstrate the important role that eddy size plays in setting the turbulent resistivity. Overall turbulent dissipation is relatively unchanged (only 15%), and yet flows are significantly more effective at field generation when the largest eddies are damped by the baffle. These results are also the first measurement of changes to the wave number resolved turbulent cascade when several modes are selectively damped and removed from the spectrum. In our analysis, we have by necessity worked with a simplified interpretation in terms of a “global α and β effect.” In fact, the nonlinear couplings

are considerably more involved, and we have considered only the largest order flows.

The authors thank Ben Brown for useful discussions and references on the role of turbulent resistivity in geophysical and astrophysical dynamo simulations and John Wallace and Paul Brooks for engineering assistance in modifying the MDE. This work is funded by the National Science Foundation and is a member experiment of the Center for Magnetic Self Organization in Laboratory and Astrophysical Plasmas.

*cbforest@wisc.edu

- [1] A. Gaillitis, O. Lielausis, E. Platacis, G. Gerbeth, and F. Stefani, *Phys. Plasmas* **11**, 2838 (2004).
- [2] R. Stieglitz and U. Müller, *Phys. Fluids* **13**, 561 (2001).
- [3] F. Ravelet *et al.*, *Phys. Rev. Lett.* **101**, 074502 (2008).
- [4] H. Moffatt, *Magnetic Field Generation in Electrically Conducting Fluids* (Cambridge University Press, Cambridge, England, 1978).
- [5] K. Krause and K.H. Rädler, *Mean Field Magnetohydrodynamics and Dynamo Theory* (Pergamon, New York, 1980).
- [6] M. Rieutord, *C.R. Physique* **9**, 757 (2008).
- [7] M. Dikpati and P.A. Gilman, *Astrophys. J.* **649**, 498 (2006).
- [8] J.-P. Laval, P. Blaineau, N. Leprovost, B. Dubrulle, and F. Daviaud, *Phys. Rev. Lett.* **96**, 204503 (2006).
- [9] K. Reuter, F. Jenko, and C. Forest, *New J. Phys.* **11**, 013027 (2009).
- [10] Y. Ponty, P. Mininni, J. Pinton, H. Politano, and A. Pouquet, *New J. Phys.* **9**, 296 (2007).
- [11] E.J. Spence, M.D. Nornberg, C.M. Jacobson, R.D. Kendrick, and C.B. Forest, *Phys. Rev. Lett.* **96**, 055002 (2006).
- [12] E.J. Spence, M.D. Nornberg, C.M. Jacobson, C.A. Parada, N.Z. Taylor, R.D. Kendrick, and C.B. Forest, *Phys. Rev. Lett.* **98**, 164503 (2007).
- [13] P. Frick, V. Noskov, S. Denisov, and R. Stepanov, *Phys. Rev. Lett.* **105**, 184502 (2010).
- [14] S.A. Colgate *et al.*, *Phys. Rev. Lett.* **106**, 175003 (2011).
- [15] M.L. Dudley and R.W. James, *Proc. R. Soc. A* **425**, 407 (1989).
- [16] E. Bullard and H. Gellman, *Phil. Trans. R. Soc. A* **247**, 213 (1954).
- [17] M. Nornberg, E. Spence, R. Kendrick, C. Jacobson, and C. Forest, *Phys. Plasmas* **13**, 055901 (2006).
- [18] F. Ravelet, L. Marié, A. Chiffaudel, and F. Daviaud, *Phys. Rev. Lett.* **93**, 164501 (2004).
- [19] P. Cortet, P. Diribarne, R. Monchaux, A. Chiffaudel, F. Daviaud, and B. Dubrulle, *Phys. Fluids* **21**, 025104 (2009).
- [20] U. Frisch, *Turbulence* (Cambridge University Press, Cambridge, England, 1995).